Thermochimica Acta, 130 (1988) 177–192
Elsevier Science Publishers B.V., Amsterdam – Printed in The Netherlands

STRUCTURAL RELAXATION AND CRYSTALLIZATION OF $Fe_{78}B_{13}Si_9$ AMORPHOUS RIBBONS STUDIED BY DILATOMETRY AND DIFFERENTIAL SCANNING CALORIMETRY

M. HARMELIN *, E. ETCHESSAHAR **, J. DEBUIGNE ** and J. BIGOT *

* *CNRS, Centre d'Etudes de Chimie Métallurgique, 15, rue Georges Urbain, 94407 Vitry-sur-Seine Cedex (France)*

** *Laboratoire de Métallurgie et Physico-Chimie des Matériaux, Institut National des Sciences Appliquées, 20, Avenue des Buttes de Coësmes, 35031 Rennes Cedex (France)*

(Received 26 October 1987)

ABSTRACT

The structural relaxation and crystallization of $Fe_{78}B_{13}Si_9$ amorphous ribbons were studied by dilatometry and differential scanning calorimetry (DSC). An own-built and highly sensitive dilatometer was used allowing samples in the form of thin ribbon to be heated at a slow heating rate (1.66 °C min^{-1}) in an ultra-high-vacuum (10^{-9} torr). Thermal expansion coefficients were determined on heating and cooling. Isothermal annealings were also performed in situ in the dilatometer at 250, 350 and 450 °C, for 2 h. The mean coefficients of linear thermal expansion ($\alpha \times 10^6$) measured between 60 and 250 °C were respectively < 5 for the as-quenched samples, 6.8 ± 0.5 for the relaxed amorphous samples (whatever the relaxation rate), and 11.8 ± 0.5 for the crystallized ones. After the first heating of the as-quenched ribbons to 250, 350 and 450 °C, structural relaxation resulted in a shrinkage of the samples which was measured after cooling to room temperature. The shrinkage of the samples increased with the temperature limit of the previous heating $< -2 \times 10^{-4}$ at 250 °C, $\sim -5 \times 10^{-4}$ at 350 °C, and $\sim -8 \times 10^{-4}$ at 450 °C. No further shrinkage of the samples was detected during the isothermal annealings at 250, 350 and 450 °C. Crystallization (between 514 and 537 °C) resulted in a more important shrinkage ($\sim -50 \times 10^{-4}$).

DSC was used for determining the relaxation rate of the specimens annealed under the same conditions as used for the the dilatometric measurements. The influence of the heating rate on the relaxation rate was also investigated. Results are interpreted by reference to models previously proposed in the literature for the structural relaxation of amorphous metallic alloys.

INTRODUCTION

Amorphous metallic alloys prepared by rapid quenching techniques are thermodynamically in non-equilibrium metastable states after quenching. Upon subsequent heating at temperatures below the beginning of crystallization they can lower their free energy continuously toward more stable (though still metastable) configurations, without crystallization. This phe-

0040-6031/88/$03.50

nomenon is called structural relaxation and is manifested by continuous changes in all physical properties. At the present time, a definitive model for structural relaxation is not yet available. Spaepen and co-workers [1,2] analyzed the structural relaxation on the basis of the free volume model: the unstable excess free volume in the as-quenched state would disappear during structural relaxation and, consequently, densification would occur. In the first approach proposed by Egami [3], structural relaxation was considered to be caused by two different processes, compositional short range ordering (CSRO) and topological short-range ordering (TSRO). Then, the defect model was proposed [4,5]. It was defined by the atomic level stresses: a small change of ~ 0.5% in the density would occur as a result of the anharmonicity of the interatomic potentials and TSRO would be explained by annihilation and recombination of the positive and negative local density fluctuations. The direct evidence by such sensitive methods as small-angle X-ray scattering, EXAFS and neutron diffraction has shown that the structural rearrangements involved during structural relaxation are extremely slight (e.g. refs. 6–8). Changes of ~ 0.5% in the density have been measured but such determinations are difficult to perform accurately and are obviously discontinuous [9–11].

Thermal expansion measurements are an interesting way to follow sample shrinkage on heating, and for determining the thermal expansion coefficients of the amorphous material in the as-quenched and relaxed state. However, until now there have been only a few experiments on measuring the changes in length during the structural relaxation and crystallization in amorphous ribbons. Such a deficiency is due to the experimental difficulties of the measurements because samples are in the form of thin ribbons and because superficial oxidation must be absolutely avoided. Moreover, a high sensitivity of the dilatometric equipment is required. Previous investigations of amorphous systems dealt with Pd–Ni–P and Pt–Ni–P alloys [9], Fe–Ni based alloys [12–19] and Ti-based alloys [20,21]. In amorphous $Ni_{78}B_{14}Si_8$ [17,18] it was shown that the shrinkage occurs rapidly at the annealing temperature above 200 °C, reaching about 0.08% in the sample annealed at 300 °C for 30 min. Assuming that $3\Delta l/l$ nearly equals the change in volume $\Delta V/V$, this value corresponds to a decrease in volume of ~ 0.24%. As pointed out by refs. 17 and 18, the disappearance and the redistribution of the excess free volume during TSRO may cause not only the densification but also the decrease in anharmonicity of the interatomic potentials.

In the Fe-based amorphous alloys, an anomaly due to the spontaneous volume magnetostriction is generally observed below the Curie temperature (T_c). The spontaneous volume magnetostriction is caused as a result of the sum of thermal, elastic and magnetic energies becoming a minimum [22]. Regarding Fe–B–Si, the thermal expansion anomaly was found to be dependent on the silicon and boron content [23], becoming more remarkable with decreasing Si or B content.

The aim of the present work is to report results obtained by carrying out precise thermal expansion measurements on $Fe_{78}B_{13}Si_9$ by using an own-built and highly sensitive dilatometer [24,25] allowing samples in the form of thin ribbon to be heated in an ultra-high vacuum. Effects of structural relaxation and crystallization were directly followed. Such direct dilatometric measurements on continuous heating are the first ones to be performed for this alloy. For this composition, Hausch and Török [26] examined the thermal expansion of $Fe_{82}B_{18-x}Si_x$ ($x = 0$, 3 and 6) but samples were stress relieved by a heat treatment at 350 °C before dilatometric measurements; Komatsu et al. [18] performed isochronal annealings on $Fe_{78}B_{14}Si_8$ in order to follow length changes during structural relaxation and crystallization, but did not determine the thermal expansion coefficients.

DSC was also used for determining the enthalpy relaxation and the crystallization temperature range of the specimens.

EXPERIMENTAL

Two amorphous ribbons (a) and (b) were used during this work. Both were prepared by planar flow casting on a copper wheel (300 mm diameter, linear speed 20 m s^{-1}). The (a) ribbon was quenched in air and the (b) ribbon in helium gas. Both were 7 mm wide and ~ 30 μm thick. These ribbons were checked by X-ray diffraction using Co $K\alpha$ radiation and a diffracted-beam graphite monochromator. No traces of Bragg peaks were detected; the results presented here were obtained from fully amorphous specimens.

Dilatometric measurements

A description of the device which was used is given elsewhere [24,25]. The specific heat treatments applied to the different samples in the dilatometer are described in Fig. 1. The length of the samples was 40 mm and a tensile stress of 5×10^4 Pa was applied to them during the experiment. The samples indicated by the letters G, I, K and M were cut off from ribbon (a) and those indicated by H, J, L and N were cut off from ribbon (b). Samples G and H were heated up to 600 °C and then cooled to room temperature at the same rate (1.66 °C min^{-1}) in order to characterize the main steps of the dimensional changes of the sample. The aim of the successive experiments performed with samples I, J, K, L, M and N was to show precise evidence of the effects of structural relaxation and of crystallization on the dilatometric behavior of the samples.

Cycle 1 was intended (i) to determine the thermal expansion of the amorphous sample heated for the first time in the as-quenched state, (ii) to determine the dimensional change during isothermal annealing (2 h at

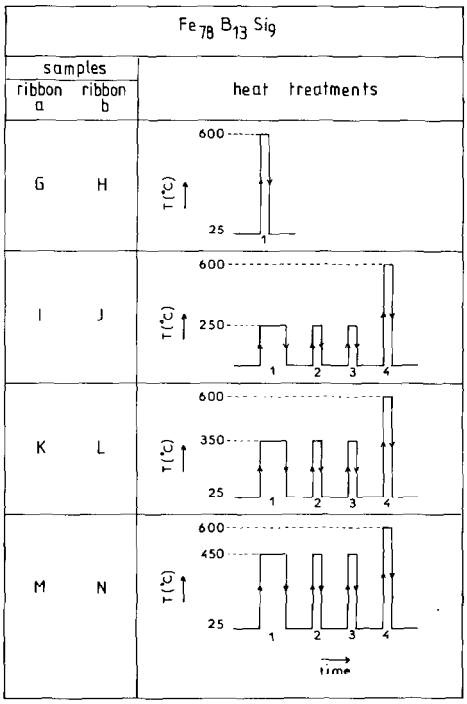

Fig. 1. Heat treatments applied to dilatometric samples cut off from amorphous $Fe_{78}B_{13}Si_9$ ribbons (a) and (b). Heating rate and cooling rate, 1.66 °C min^{-1}; annealing time at 250, 350 and 450 °C, 2 h for cycle 1, 5 min for cycles 2 and 3; annealing time at 600 °C, 1 min.

250 °C for samples I and J, at 350 °C for samples K and L and at 450 °C for samples M and N), (iii) to compare the thermal expansion on heating and cooling, and (iv) to compare the sample length before and after the complete cycle.

Cycle 2 was intended to determine the thermal expansion of the sample in the relaxed state obtained after the cycle 1,

Cycle 3 was intended to check the reproducibility of the results obtained during the cycle 2,

Cycle 4 was intended to investigate the amorphous–crystal transition.

Calorimetric measurements

A Perkin-Elmer Differential Scanning Calorimeter (DSC-2C) connected to a 3600 Thermal Analysis Data Station was used for the calorimetric measurements. Each specimen (~ 20 mg) was enclosed in a copper pan. Crystallized samples were used as a reference. The atmosphere was pure argon. The relaxation enthalpy of each specimen was measured by integrating the area between the curve obtained on heating the specimen for the first time (for instance traces (a) in Figs. 5 and 7) and the curve obtained on

heating the same specimen a second time (traces (b) in Figs. 5 and 7). The first heating stopped at 500 °C, just before crystallization occurs, the specimen being then rapidly cooled to room temperature. Trace (b) is a reference curve, strictly reproducible for all specimens. It corresponds to a relaxed and prestabilized state under the conditions of the heat treatments used (heating rate 80 °C min^{-1}, cooling rate 320 °C min^{-1}).

DILATOMETRIC RESULTS

An example of the dilatometric curve obtained with sample G on continuous heating and cooling is shown in Fig. 2. Evidence is given of the thermal expansion, the Curie temperature and of the crystallization of the amorphous sample on heating. On cooling, the behavior of the crystallized sample is linear without discontinuity. Comparison of the dilatometric curves obtained with sample I ($T_a = 250$ °C), sample K ($T_a = 350$ °C) and sample N ($T_a = 450$ °C) is shown in Fig. 3. The values of the residual shrinkage measured at room temperature with the samples annealed at 250, 350 and 450 °C and with those crystallized after heating at 600 °C are given in Table 1. The following features can be observed: (i) during the first heating of the

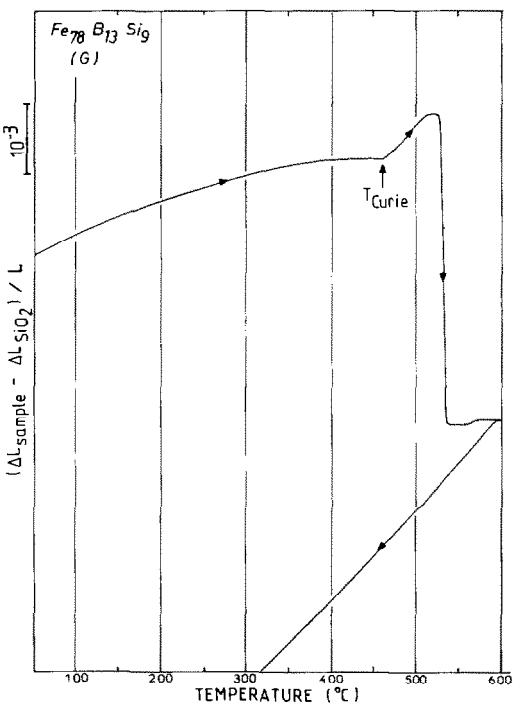

Fig. 2. Dilatometric curve obtained with sample G on heating and cooling.

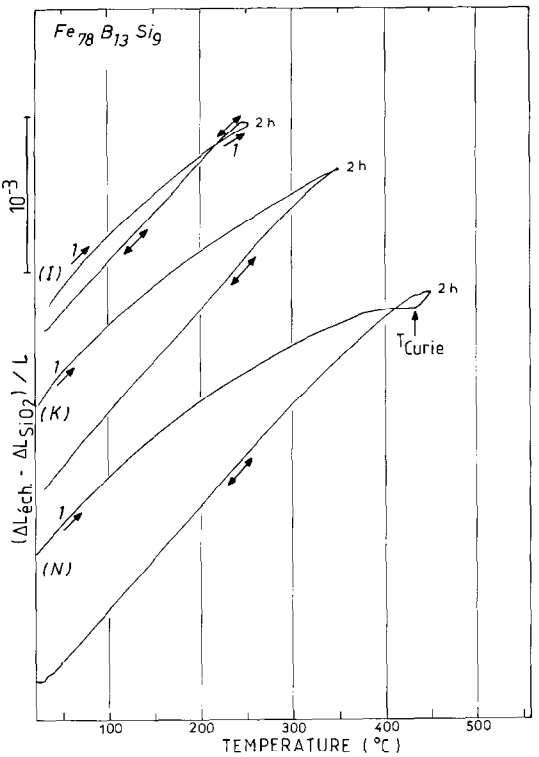

Fig. 3. Dilatometric curves obtained with samples I, K and N during cycle 1 as described in Fig. 1.

TABLE 1

Residual shrinkage measured at 25 °C after cycles 1, 2, 3 and after crystallization of the amorphous $Fe_{78}B_{13}Si_9$ alloy

Sample	No.	Annealing temperature (°C)	$\Delta l/l$ ($\times 10^{-4}$)			
			Cycle 1	Cycle 2	Cycle 3	Crystallization (514–537 °C)
G	2	–	–	–	–	−43.2
H	1	–	–	–	–	−49.6
I	1	250	−1.6	0	0	−49.0
J	1	250	−0.6	−0.5	0	−51.6
K	1	350	−5.3	0	0	−46.2
L	1	350	−5.1	0	0	−48.6
M	2	450	−8.3	−0.5	−0.1	not measured
N	2	450	−8.2	0	0	not measured

No. = number of strips used for the experiment.

as-quenched sample, change in the sample length is not linear; (ii) during the isothermal annealing, only a very small creep is observed at 250 and 350 °C, and no change in length at 450 °C. Thus, no major shrinkage is detected during isothermal annealing; (iii) on cooling, the dilatometric curves are linear below ~ 400 °C; (iv) a residual shrinkage is detected at room temperature after cycle 1, and the extent of the shrinkage increases as the annealing temperature is increased. With the exception of samples J and M, no more shrinkage is observed during cycles 2 and 3; (v) the cooling curves obtained after cycle 1 are strictly reproducible with those obtained during cycles 2 and 3; (vi) the heating curves obtained with cycles 2, 3 and 4 are strictly reproducible below crystallization; (vii) the cooling curves during cycles 1, 2 and 3 are well reproducible with those obtained on heating during cycles 2, 3 and 4 below crystallization. There exist only very small variations attributed to the dilatometric equipment.

Thus, it can be concluded that, under conditions of the low heating rates which were used (1.66 °C min^{-1}), the sample length was almost in complete equilibrium on heating in the whole range of temperature of the structural relaxation. Using the relation of $3\Delta l/l = \Delta V/V$, where $\Delta l/l$ is the length change and $\Delta V/V$ is the volume change, in order to estimate the volume change (densification) from the length change, there is a change of − 0.25% for structural relaxation after heating to 450 °C and − 1.44% after crystallization at 600 °C. These values are of the same order as those reported by Komatsu et al. [18], respectively 0.15 and 1.61% for $Fe_{78}B_{14}Si_8$ after isochronal annealings (30 min) up to 450 and 600 °C.

Regarding the results reported by Bothe et al. [19] for $Fe_{32}Ni_{36}Cr_{14}P_{12}B_6$ which were obtained after successive isochronal annealings, in spite of an apparent agreement between the respective values of the shrinkage for corresponding temperatures, the kinetics of shrinkage are very different. Though almost identical heating rates were used for attaining the annealing temperatures (2 °C min^{-1} for Bothe et al. and 1.66 °C min^{-1} in this work), no shrinkage was observed on heating by Bothe et al., but increasing shrinkage with time was observed during the isothermal annealing. Because their samples were heated in argon, this unexpected increase of shrinkage with annealing time might be due to some superficial oxidation of the samples.

The values of the average linear thermal expansion coefficients α measured with the different samples between room temperature and 250 °C are given in Table 2. It can be concluded that (i) the α values are the same for the (a) and (b) ribbons and remain unaffected by the number of strips used for the experiment; (ii) the α values of the first heating of the as-quenched sample (cycle 1) are smaller than those measured on cooling or during the other successive heatings; (iii) a small difference is observed between the values measured on heating and cooling during cycles 2, 3 and 4 (below crystallization): $(6.5 \pm 0.2) \times 10^{-6}$ and $(7.0 \pm 0.1) \times 10^{-6}$, respectively. This

TABLE 2

Mean coefficients of linear thermal expansion $\alpha = (l_{250} - l_{60}/l_{60}) \times 10^{-6}$ of the amorphous $Fe_{78}B_{13}Si_9$ alloy

Sample	No.	Heating				Cooling			
		Cycle 1	Cycle 2	Cycle 3	Cycle 4	Cycle 1	Cycle 2	Cycle 3	Cycle 4
G	2	–	–	–	–	*11.9*	–	–	–
H	1	–	–	–	–	*12.0*	–	–	–
I	1	< 5	6.38	6.16	6.26	6.81	6.63	6.55	*13.0*
J	1	< 5	6.30	6.23	6.20	6.74	6.66	6.87	*11.7*
K	1	< 5	6.58	6.59	6.58	7.24	7.15	7.04	*11.3*
L	1	< 5	6.56	6.50	6.59	6.96	6.89	7.08	*11.6*
M	2	< 5	6.57	6.25	n.m.	6.91	7.34	7.11	n.m.
N	2	< 5	6.67	6.73	6.71	7.25	7.40	7.40	*11.3*

Average values for the as-quenched amorphous state on heating were < 5; for the relaxed amorphous state on heating 6.5 ± 0.2 and on cooling 7.0 ± 0.1; and for the crystallized state on cooling 11.8 ± 0.5. Values in italics indicate the crystallized state, and n.m. indicates not measured.

difference is probably artificial and due to some defect of the dilatometric device. Thus, we propose the mean value $\alpha = (6.8 \pm 0.5) \times 10^{-6}$ as the most representative one for the relaxed amorphous $Fe_{78}B_{13}Si_9$ alloy; (iv) in the temperature range below the annealing temperature, the α values of the relaxed amorphous sample remain unaffected by the relaxation extent. However, the samples annealed at 350 °C are more relaxed than those annealed at 250 °C, and the samples annealed at 450 °C are more relaxed than those annealed at 350 °C. This fact reveals that the shrinkage (densification) mechanisms are irreversible; (v) the α value of the crystallized sample is higher than that of the relaxed sample: the average value equals

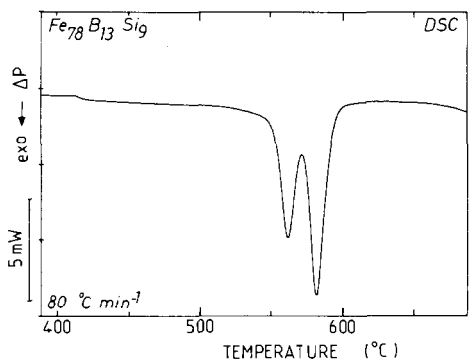

Fig. 4. Typical DSC curve between 400 and 680 °C showing the Curie temperature (413 °C) and the two stages of crystallization of the amorphous $Fe_{78}B_{13}Si_9$ alloy. The curve is normalized to 1 mg sample weight.

11.8×10^{-6}. It is worth noting that this value depends on the relative proportions of the crystallized phases formed during the crystallization process. As a matter of fact, as was shown in ref. 30 by DSC, X-ray diffraction and electron microscopy, amorphous $Fe_{78}B_{13}Si_9$ crystallizes in two main stages (Fig. 4). The first one gives a mixture of the equilibrium phase α-Fe and of the metastable one $Fe_3(Si, B)$; the second one corresponds to the transformation of the metastable phases into stable ones (mainly Fe_2B). As shown in Fig. 2, the first stage is revealed by a sharp shrinkage in the dilatometric curve while the second one, which corresponds mainly to small atomic rearrangements, does not so much affect the thermal expansion of the sample.

DSC RESULTS

DSC experiments were performed in order to determine the enthalpy changes corresponding to the heat treatments applied during the dilatometric investigations, and thus to provide evidence of structural rearrangements on continuous heating of the as-quenched samples or after isothermal annealings, even when no corresponding changes were measured on the dilatometric curves. For this purpose, two kinds of heat treatments were applied to the DSC samples: (1) a series of as-quenched samples was heated slowly up to the annealing temperature (T_a) at a heating rate (1.25 °C min^{-1}), approximately the same as that used for the dilatometric measurements (1.66 °C min^{-1}). After 1 min at T_a, they were rapidly cooled to room temperature. Then they were heated again in the DSC cell at 80 °C min^{-1} twice to 500 °C; (2) another series of as-quenched samples was annealed in a furnace (under ultra-high-vacuum) for 2 h at T_a. After cooling to room temperature, the annealed samples were heated again in the DSC cell twice to 500 °C, in the same way as the samples annealed for 1 min at the same value of T_a. This procedure allowed us to determine and to compare the enthalpy changes and the Curie temperatures of the samples annealed for 1 min or 2 h at a given value of T_a (here 250, 350 and 450 °C). Similar results were obtained with ribbons (a) and (b). Examples of the corresponding DSC curves are given in Fig. 5. Results are summarized in Table 3.

Figure 5 shows typical DSC curves obtained with specimens in the as-quenched state and annealed at 250, 350 and 450 °C for 1 min and 2 h. For the as-quenched specimens, an exothermic phenomenon was detected during the first scan (trace (a)), starting at ~ 180 °C up to the beginning of crystallization (520 °C). In order to measure the corresponding heat effect, heating was stopped at 500 °C in this series of experiments. This exothermic phenomenon was irreversible on cooling and the second scan (trace (b)) delimited an area proportional to the relaxation enthalpy of the specimen (32 J g^{-1}). After annealing for 1 min at 250 °C, the exothermic effect was

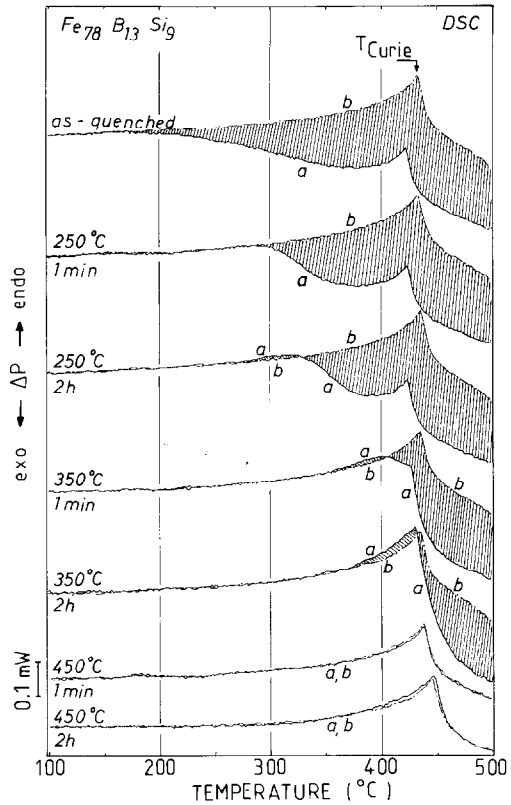

Fig. 5. DSC curves of amorphous $Fe_{78}B_{13}Si_9$ samples in the as-quenched state and after annealing for 2 hours at 250, 350 and 450 °C. Trace (a): first heating up to 500 °C. After a rapid cooling (320 °C min^{-1}) to room temperature, the same sample was heated again in the same conditions (trace (b)). The shaded area is proportional to the relaxation enthalpy. Curves are normalized to 1 mg sample weight; heating rate, 80 °C min^{-1}.

eliminated below 250 °C, and the residual exothermic effect began at ~ 290 °C. The corresponding enthalpy change measured up to 500 °C was 26 J g^{-1} and the Curie temperature was the same as that of the as-quenched specimen. After annealing for 2 h at 250 °C, the residual exothermic effect began at 320 °C and the corresponding enthalpy change was 23 J g^{-1}. The Curie temperature remained unchanged by comparison with the as-quenched state.

After annealing for 1 min at 350 °C, the exothermic effect was eliminated below 350 °C, and a small endothermic peak (reversible) [11,27–29] appeared above 350 °C and up to 400 °C. It was followed by a residual exothermic effect beginning at 400 °C. The corresponding enthalpy change measured from 400 to 500 °C was 12.6 J g^{-1} and the Curie temperature remained practically unchanged compared with the as-quenched state. After annealing for 2 h at 350 °C, the endothermic peak above 350 °C remained

TABLE 3

Influence of the annealing conditions on the enthalpy relaxation and the Curie temperature of the amorphous $Fe_{78}B_{13}Si_9$ alloy (heating rate 80 °C min^{-1})

Annealing conditions			Relaxation enthalpy [a]		Curie temperature [a] (°C)
Temperature T_a (°C)	Heating rate up to T_a (°C min^{-1})	Time at T_a	T_i (°C)	$\Delta H_{T_i}^{500\,°C}$ (J g^{-1})	
250	1.25	1 min [b]	290	26	413.3
	n.m.	2 h [c]	320	23	413.3
350	1.25	1 min [b]	400	12.6	+2.5
	n.m.	2 h [c]	430	8.5	+5.0
450	1.25	1 min [b]	–	0	+2.0
	n.m.	2 h [c]	–	0	+16.0
As-quenched samples			180	32	413.3

[a] Results were strictly the same for ribbons (a) and (b).
[b] These samples were annealed in the DSC cell.
[c] These samples were annealed in an ultra-high-vacuum furnace. n.m. = not measured.

small but nevertheless greater than after 1 min at 350 °C: the residual exothermic effect began at 430 °C. The corresponding enthalpy change measured from 430 to 500 °C was 8.5 J g^{-1} and the Curie temperature was 5 °C higher than that measured with samples in the as-quenched state.

After annealing for 1 min and 2 h at 450 °C, the exothermic effect was completely eliminated up to 500 °C. Thus the effect of annealing for 2 h at 450 °C could not be measured by DSC. However, the great enhancement of the Curie temperature (+2 °C after 1 min and +16 °C after 2 h) indicates that compositional short-range ordering probably occurred during the isothermal treatment.

Thus, clear evidence is given by the DSC curves that structural rearrangements occur during isothermal treatment for 2 h at 250 and 350 °C, especially at 350 °C. This structural relaxation does not correspond to any shrinkage of the samples, as shown by the dilatometric curves, and may be expected to correspond to compositional short range ordering.

Influence of the heating rate

As the heating rate used for the dilatometric measurements was much smaller than that used for the DSC experiments, the influence of the heating rate used for attaining the annealing temperature T_a was systematically investigated by DSC from 1.25 to 320 °C min^{-1}. For these experiments, T_a = 350 °C. The procedure is described in Fig. 6. ΔT is the time elapsed on heating each sample from room temperature (50 °C) to the annealing

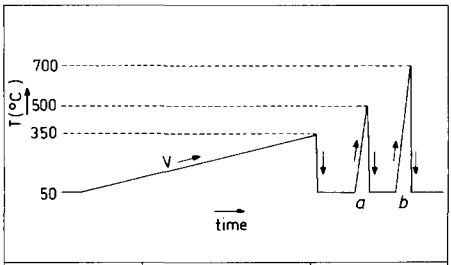

V (°C min^{-1})	Δt (seconds) 350° / 50	a, b
320	56	Heating rate : 40°C min^{-1}
160	112	
80	225	
40	450	
20	900	
10	1800	Cooling rate : 320°C min^{-1}
5	3600	
2.5	7200	
1.25	14400	

Fig. 6. Heat treatments applied to DSC samples in order to study the influence of the heating rate V used for attaining the annealing temperature T_a on the enthalpy relaxation and the Curie temperature of amorphous $Fe_{78}B_{13}Si_9$ samples. Here $T_a = 350\,°C$ and $t_a = 1$ min.

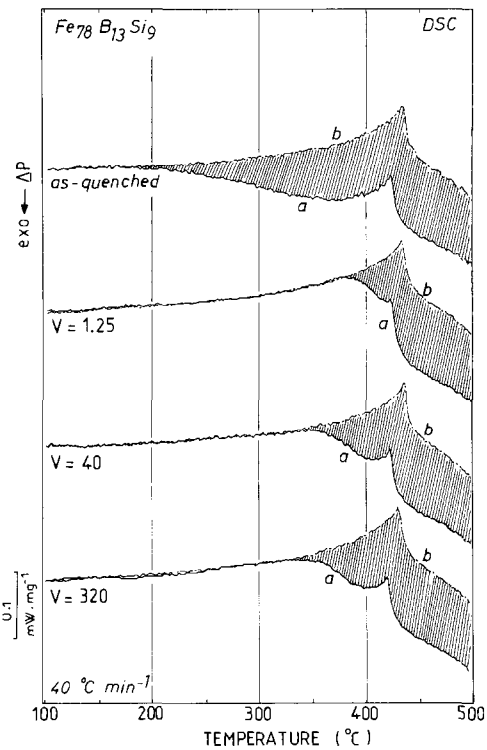

Fig. 7. Typical DSC curves obtained after annealing for 1 min at 350 °C when different heating rates V were used for attaining 350 °C. Here V = 1.25, 40 and 320 °C as described in Fig. 6. The shaded area is proportional to the residual enthalpy relaxation. Sample weight, 20 mg; heating rate, 40 °C min^{-1}.

TABLE 4

Effect of the heating rate V_a used for attaining the annealing temperature T_a on the enthalpy relaxation and the Curie temperature of amorphous $Fe_{78}B_{13}Si_9$ samples annealed for 1 min and 2 h at T_a

Annealing conditions (T_a = 350 °C)		Enthalpy relaxation $\Delta H_{T_i}^{500\,°C}$ (±0.5) (J g^{-1})	Variation of the Curie temperature (±0.5) (°C)
V_a (°C min^{-1})	Time at T_a		
320	1 min	20.2	0
160	1 min	19.7	+0.2
80	1 min	20.5	+0.8
40	1 min	20.3	+0.2
20	1 min	19.7	+0.6
10	1 min	19.9	+0.7
5	1 min	17.8	+1.6
2.5	1 min	17.5	+0.6
1.25	1 min	16.6	+0.9
80	2 h	10.7	+6.1
1.25	2 h	9.9	+5.8

Anneals for 1 min and 2 h were both performed in the DSC cell. Heating rate 40 °C min^{-1}.

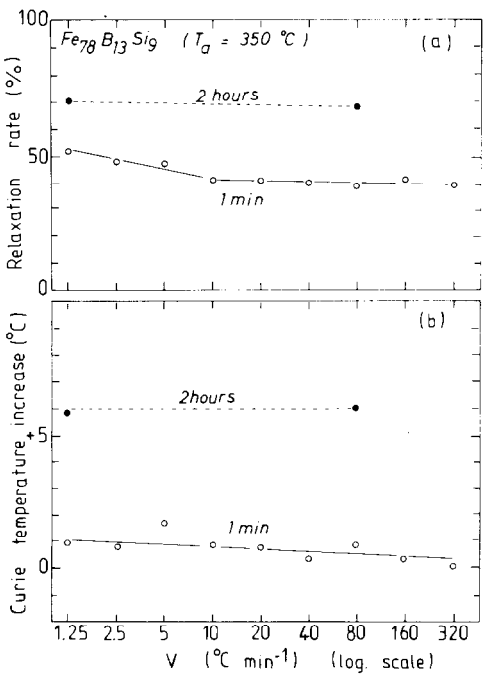

Fig. 8. Influence of the heating rate V used for attaining the annealing temperature (here T_a = 350 °C) on the relaxation rate and the Curie temperature (413 °C for the as-quenched ribbon) of amorphous $Fe_{78}B_{13}Si_9$ samples. Comparison between the results obtained with t_a = 1 min and 2 h at T_a = 350 °C. A logarithmic scale is used for V for the sake of clarity of results in the range of the small values of V.

temperature (350 °C) for each value of heating rate V from 1.25 to 320 °C min^{-1}. Examples of the corresponding DSC curves are illustrated in Fig. 7 for V = 1.25, 40 and 320 °C min^{-1}. The final results are given in Table 4 and Fig. 8.

Figure 7 shows typical DSC curves obtained by heating at 40 °C min^{-1} samples previously heated up to 350 °C in the DSC cell with increasing heating rates (V = 1.25, 40, 320 °C min^{-1}) and annealed for 1 min at 350 °C before being rapidly cooled. The higher the heating rate up to 350 °C, the less relaxed is the sample, since the shaded area corresponding to the relaxation heat evolved during the measurement at 40 °C min^{-1} is greater. The endothermic effect observed on the DSC curves after 2 h at 350 °C did not appear for these samples annealed only for a very short time at 350 °C. Thus, it may be concluded that compositional short range order was avoided because it did not have enough time to be established. That is confirmed by Table 4 and Fig. 8 which show that the Curie temperature remained practically unchanged within experimental error (±0.5 °C). On the other hand, after 2 h at 350 °C the relaxation rate, measured by the decrease of the amplitude of the initial exothermic effect, had increased, an endothermic effect above 350 °C had developed (see Fig. 5) and the Curie temperature had increased (~ +6 °C). Thus, these results also clearly show that a structural evolution occurred during the 2-h isothermal treatment, and that evolution did not correspond to any shrinkage of the samples. The corresponding structural evolution probably involves very slight atomic rearrangements of the amorphous structure, and consequently does not modify the density of the sample.

CONCLUSIONS

During the first heating of amorphous ribbons in the as-quenched state two phenomena are superimposed: (i) the usual thermal expansion of the alloy, and (ii) the shrinkage of the amorphous sample due to the annealing-out of the excess free volume. From comparison between thermal expansion and DSC measurements, it was concluded that the annealing-out of the excess free volume explains the densification of the sample and contributes mainly to the exothermic effect detected on the DSC curves during the first heating of the as-quenched samples. The time constant of this process is small (~ 1 s). This explains why such high heating rates as 40 or 80 °C min^{-1} used in the DSC technique are able to determine with a good approximation the relaxation rate of the as-quenched samples.

With slow heating rates such as those used for the dilatometric experiments described in this paper (~ 2 °C min^{-1}), equilibrium was attained at each temperature and no further shrinkage occurred during isothermal annealings. After the first heating of the as-quenched sample (without

crystallization) the thermal expansion coefficient of the amorphous alloy remains constant up to 400 °C: $\alpha = (6.8 \pm 0.5) \times 10^{-6}$. Above 400 °C, the Curie temperature results in a magnetostriction effect. The value of α remains unaffected by the relaxation rate of the sample.

The thermal expansion coefficient of crystallized $Fe_{78}B_{13}Si_9$ is $\alpha = (11.8 \pm 0.5) \times 10^{-6}$, i.e. higher than that of the amorphous alloy. However, as the crystallized alloy is a mixture of several phases (α-Fe, Fe_3B and Fe_2B) [30] this result cannot be considered as a general one and the value of α of the crystallized alloy may possibly vary with the composition of the mixture which depends on the heating rate.

The residual shrinkage observed at room temperature by cycling the amorphous material from different temperatures (250, 350 and 450 °C) increased with the temperature limit. The maximum value was attained at 450 °C corresponding to $\Delta V/V = -0.08\%$; this value was of the same order as that reported by Komatsu et al. [17] with a paramagnetic alloy but a lower temperature (300 °C).

This series of results allows us to conclude that the major part of the irreversible exothermic effect detected by DSC during the first heating of the as-quenched samples corresponds to the progressive shrinkage of the sample measured on the dilatometric curves. This phenomenon would also correspond in major part to the annealing-out of the excess free volume and to the establishment of TSRO, in agreement with our previous neutron diffraction experiments [8].

Comparison between dilatometric and DSC experiments also provides evidence that compositional short-range ordering probably occurs during isothermal annealings but does not result in any dimension change of the sample. That can be easily understood, as the atomic rearrangements involved are extremely slight [7,8].

ACKNOWLEDGMENTS

This work was supported by CNRS, IMPHY S.A. and USINOR in the framework of the Groupement Scientifique Matériaux Amorphes.

REFERENCES

1 A.I. Taub and F. Spaepen, Acta Metall., 28 (1980) 1781.
2 S.S. Tsao and F. Spaepen, in T. Masumoto and K. Suzuki (Eds.), Proceedings of the 4th International Conference on Rapidly Quenched Metals, The Japan Institute of Metals, Sendai, 1982, Vol. I, p. 463.
3 T. Egami, Mater. Res. Bull., 13 (1978) 557.
4 D. Srolovitz, K. Maeda, V. Vitek and T. Egami, Phil. Mag. A, 44 (1981) 847.
5 T. Egami and V. Vitek, J. Non-Cryst. Solids, 61&62 (1984) 499.

6 M. Harmelin, A. Naudon, J.M. Frigerio and J. Rivory, in S. Steeb and H. Warlimont (Eds), Rapidly Quenched Metals, Vol. II, North-Holland, 1985, p. 659.
7 M. Harmelin, A. Sadoc, A. Naudon, A. Quivy and Y. Calvayrac, J. Non-Cryst. Solids, 74 (1985) 107.
8 S. Lefebvre, M. Harmelin, A. Quivy, J. Bigot, Y. Calvayrac and R. Bellissent, Z. Phys. Chem. N. F., 157 (1988) S365.
9 H.S. Chen, J.T. Krause and E.A. Sigety, J. Non-Cryst. Solids, 13 (1973/74) 321.
10 H.S. Chen, J. Appl. Phys., 49 (1978) 3289.
11 M. Harmelin, Y. Calvayrac, A. Quivy, J. Bigot, P. Burnier and M. Fayard, J. Non-Cryst. Solids, 61&62 (1984) 931.
12 H.A. Brooks, J. Appl. Phys., 49 (1978) 213.
13 J.E. Shelby, J. Non-Cryst. Solids, 34 (1979) 111.
14 J. Steinberg, S. Tyagi and A.E. Lord, Jr., J. Non-Cryst. Solids, 41 (1980) 279.
15 A. Kuršumović, R.W. Cahn and M.G. Scott, Scripta Metall., 14 (1980) 1245.
16 A. Kuršumović, E. Girt, E. Babić, B. Leontić and N. Njuhović, J. Non-Cryst. Solids, 44 (1981) 57.
17 T. Komatsu, M. Takeuchi, K. Matusita and R. Yokota, J. Non-Cryst. Solids, 57 (1983) 129.
18 T. Komatsu, K. Matusita and R. Yokota, J. Non-Cryst. Solids, 69 (1985) 347.
19 K. Bothe, M. Hansmann and H. Neuhauser, Scripta Metall., 19 (1985) 1513.
20 G. Fritsch, P. Löbl and E. Löscher, in S. Steeb and H. Warlimont (Eds.), Rapidly Quenched Metals, Vol. II, North-Holland, 1985, p. 1027.
21 P. Duhaj, G. Vlasak and P. Svec, in S. Steeb and H. Warlimont (Eds.), Rapidly Quenched Metals, Vol. II, North-Holland, 1985, p. 767.
22 K. Fukamichi, in F.E. Luborsky (Ed.), Amorphous Metallic Alloys, Butterworth, London, 1983, p. 317.
23 M. Kikuchi, K. Fukamichi and T. Masumoto, Sci. Rep. Res. Inst. Tohoku Univ., A26 (1977) 232.
24 E. Etchessahar, D. Ansel and J. Debuigne, Mém. Sci. Revue Métall., 74 (1977) 469.
25 E. Etchessahar and J. Debuigne, to be published.
26 G. Hausch and E. Török, in S. Steeb, H. Warlimont (Eds.), Rapidly Quenched Metals, Vol. II, North-Holland, 1985, p. 1341.
27 A.L. Mulder, Selected properties of some metallic glasses, Thesis, Utrecht, 1983.
28 A. Inoue, T. Masumoto and H.S. Chen, J. Mater. Sci., 19 (1984) 3953.
29 Z. Altounian, J.O. Strom-Olsen and M. Olivier, J. Mater. Res., 2 (1987) 54.
30 J. Devaud-Rzepski, A. Quivy, M. Harmelin, J.-P. Chevalier and Y. Calvayrac, in M.D. Baro and N. Clavaguera (Eds.), Proceedings of the First International Workshop on Non-Crystalline Solids, World Scientific Publ. Co., 1986, p. 231.